Interaction of Bombolitin III with Phospholipid Monolayers and Liposomes and Effect on the Activity of Phospholipase A_2†

Giovanni Signor,‡ Stefano Mammi,‡ Evaristo Peggion,*,‡ Helmut Ringsdorf,§ and Alice Wagenknecht§

University of Padova, Department of Organic Chemistry, Biopolymer Research Center, Via Marzolo 1, 35131 Padova, Italy, and Institut fur Organische Chemie der Universität Mainz, J. J. Becher Weg 18-20, D-6500 Mainz, Germany

Received November 10, 1993; Revised Manuscript Received March 17, 1994®

ABSTRACT: This study is focused on the characterization of the interaction of the amphiphilic peptide bombolitin III (from the bumblebee *Megabombus pennsylvanicus*) with phospholipid monolayers and vesicles. It is shown that due to the amphiphilic character of its α-helical conformation this water-soluble peptide is able to interact in an ordered fashion with phospholipid organized structures. Depending on the temperature, the subphase, and the particular phosphatidylcholine used, the mixed peptide–phospholipid monolayers can be homogeneous or display phase separation. This behavior was observed by means of the Langmuir film balance technique, coupled with an epifluorescence microscope. In well-defined conditions it is possible to visualize the formation of phase-separated peptide domains at the air–water interface and to study the effect of their presence on the organization of the lipid. The action of phospholipase A_2 at the lipid–peptide interface was also followed by means of fluorescence microscopy: some evidence that the enzyme preferentially hydrolyzes the phospholipid that is in contact with the peptide is presented. Furthermore, the presence of bombolitin III in L-α-DLPC monolayers causes an increase in the initial speed of degradation with phospholipase A_2. These results are in agreement with previous findings that show that the bombolitins are activators in vitro of phospholipase A_2. Experiments were also performed with peptide fragments corresponding to the α-helical sequences of the protein uteroglobin: despite some amphiphilic character, these peptides do not interact strongly with phospholipid monolayers. Only one of these peptides (corresponding to the helix 4-14 in uteroglobin) is adsorbed in the monolayer in a similar fashion to bombolitin III but does not cause an increase in the activity of phospholipase A_2.

The bombolitins are a family of five heptadecapeptides isolated from the venom of the bumblebee *Megabombus pennsylvanicus* (Argiolas & Pisano, 1985). Their biological characterization in vitro has shown that they are membrane active peptides, capable of lysing erythrocytes and liposomes and increasing the activity of the enzyme phospholipase A_2 (Argiolas & Pisano, 1985). In more general terms the bombolitins share common biological properties with other "toxin" peptides such as melittin, crabrolin, and mastoparans. All of these peptides have different amino acids sequences but are able to form amphiphilic α-helical structures either by self-association or by interaction with amphiphilic matrices such as micelles or vesicles. The biological activity of these peptides seems then to be directly correlated to their capability to form an amphiphilic order structure (α-helix) that allows them to associate and penetrate cellular membranes (Kaiser & Kezdy, 1983).

Recently, the conformational behavior of two of the bombolitins (I and III) was investigated by means of circular dichroism and ^{1}H-NMR techniques (Bairaktari et al., 1990a,b). The results of those studies showed that both peptides assume an α-helical conformation in the presence of SDS micelles (with a content of α-helix between 60 and 70%). Bombolitin III is also capable of forming an α-helical structure in water by self-association.

We decided to extend these studies by investigating the interaction of bombolitin III (see Table 1 for the peptide sequence and helical wheel diagram) with phospholipid monolayers and liposomes, clearly a better model for biological membranes. In particular, we have used an epifluorescence microscope coupled with a Langmuir film balance; this technique has recently proven to be very useful in visualizing the action of the enzyme phospholipase A_2 on phospholipid monolayers of different compositions and in different physical states (Ahlers et al., 1990; Grainger et al., 1989, 1990a; Reichert et al., 1992). Our results show for the first time that it is also possible to visualize the presence of the peptide in the monolayer. We believe this will be useful to gain insight on the interaction between the peptide and the components of the membrane, and moreover it might clarify whether the modulation of PLA_2[1] activity by bombolitins and other peptides reflects an effect on the physical state of the membrane or a direct interaction with the enzyme.

MATERIALS AND METHODS

Materials. Bombolitin III and uteroglobin fragments were obtained by solid-phase synthesis procedures and purified by HPLC. The final products exhibited single peaks in the HPLC profile with different eluting systems. The primary structure of the peptides was confirmed by amino acid analysis (with both enzymatic and acid hydrolysis), mass spectroscopy, and Edman automatic sequencing. Peptide solutions were prepared from the lyophilized peptide (peptide content of the powder was 63% in weight from amino acid analysis for bombolitin III and 68% for uteroglobin fragment 4-14).

† This work was supported in part by the National Research Council of Italy. G.S. was supported by a CNR fellowship.

* Author to whom correspondence should be addressed.
‡ University of Padova.
§ Universität Mainz.

® Abstract published in *Advance ACS Abstracts,* April 15, 1994.

[1] Abbreviations: BIII, bombolitin III; L-α-DPPC, L-α-dipalmitoylphosphatidylcholine; L-α-DMPC, L-α-dimyristoylphosphatidylcholine; L-α-DSPC, L-α-distearoylphosphatidylcholine; L-α-DLPC, L-α-dilauroylphosphatidylcholine; Tris, tris(hydroxymethyl)aminomethane; PLA_2, phospholipase A_2; CD, circular dichroism.

0006-2960/94/0433-6659$04.50/0

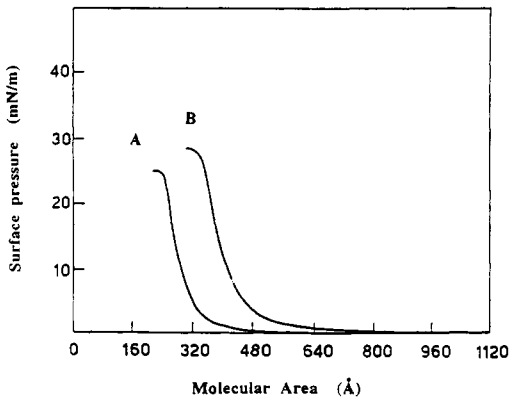

FIGURE 1: Surface pressure/area isotherms of a monolayer of pure bombolitin III. The peptide was spread on the aqueous subphase from a stock solution in $CHCl_3$–MeOH (60:40). The subphase consists of (A) Millipore water, pH 5.0; (B) buffer 10 mM Tris, 20 mM NaCl, 0.5 mM $CaCl_2$, pH 8.0.

Phospholipase A_2 (*N. naja naja* and porcine pancreas), L-α-DLPC, L-α-DMPC, L-α-DPPC, and L-α-DSPC were purchased from Sigma. Fluorescein isothiocyanate was purchased from Aldrich, and the fluorescent lipid probe SR-DPPE was purchased from Molecular Probes. This lipid (SR-DPPE) was shown by monolayer measurements to partition preferentially into the fluid phase of lipid monolayers. All phospholipids were used as supplied after their purity was checked by TLC analysis. The procedure of fluorescent labeling of PLA_2 with fluorescein isothiocyanate has been described previously in detail (Grainger et al., 1989, 1990a). All buffers for the water subphase in the Langmuir film balance experiments were prepared from Millipore water (18-MΩ resistivity) and reagent grade Tris, NaCl, and $CaCl_2$.

Methods. Circular dichroism spectra were obtained on a Jasco Model J-600A automatic recording spectropolarimeter interfaced and controlled by a PC. The measurements were performed at 25 °C in quartz cells of 0.1 cm. Multiple scans were obtained to improve the signal to noise ratio. All CD spectra are reported in terms of ellipticity units per mole of peptide residue.

Small unilamellar vesicles (SUV) were prepared following standard methods available in the literature (Szoka & Papahadjopoulos, 1980; Wallace & Blout, 1979; Wallace et al., 1981). The lipid was dissolved in spectroscopic grade $CHCl_3$ (44.22 mg in 10 mL), and this solution was evaporated in a glass tube using a rotary evaporator (to deposit the lipid as a thin film on the glass walls). The dry lipid was redissolved in Millipore water (10 mL) and the milky suspension sonicated until the turbidity (at 400 nm) had reached a constant minimum value. The sonication was performed in the case of L-α-DMPC at a temperature between 25 and 30 °C, i.e., above the phase transition temperature. After sonication, the solution was filtered with a 0.45-μm Millipore filter to remove most of the bigger liposomes and then used directly for the CD measurements. The filtration step was shown not to influence the behavior of the peptide and its association with the vesicles, but it considerably reduces the light scattering phenomena, thus improving the CD signal to noise ratio (Litman, 1972). The peptide was added to the vesicle solution, after the sonication step, from a stock solution in water (0.2275 mM). Final concentration of the peptide solutions used to record the spectra was 22.75 μM. The lipid:peptide ratio was varied by previous dilution of the stock solution of the sonicated vesicles.

The experiments with giant liposomes were performed in a temperature-controlled flow chamber (volume 200 μL), in

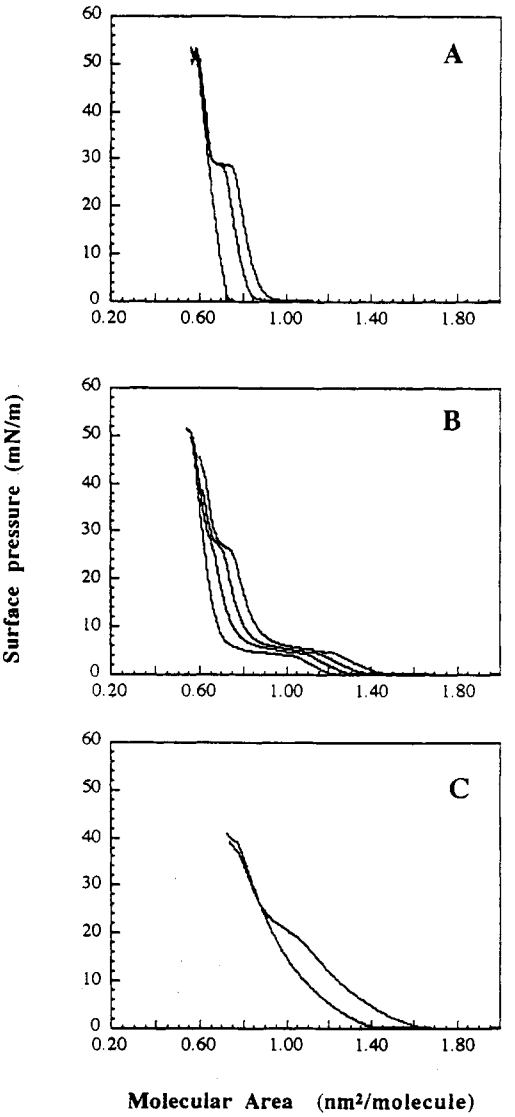

FIGURE 2: Surface pressure/area isotherms of monolayers of L-α-DPPC, at different temperatures, on bombolitin III solutions at different concentrations in Millipore water. In the absence of the lipid the peptide solutions did not display any measurable surface pressure. (A) Temperature 10 °C; from left to right the isotherms correspond to 0, 30, and 60 nM bombolitin III. (B) Temperature 20 °C; from left to right the isotherms correspond to 0, 15, 25, and 35 nM bombolitin III. (C) Temperature 40 °C; from left to right the isotherms correspond to 0 and 30 nM bombolitin III.

which the giant liposomes were prepared directly by hydration of a lipid film deposited on a glass slide by evaporation of a chloroform solution. By using a step-motor controlled syringe, the medium could be gradually modified and additional components could be injected. The observation of the liposomes was carried out with an inverse phase contrast microscope (Ringsdorf et al., 1988).

A description of the epifluorescence microscope and associated Langmuir film balance has been published elsewhere (Grainger et al., 1989; Meller, 1988). Discrimination of excitation and emission from the different fluorescence probes is regulated by conventional dichroic mirrors and interchangeable cutoff filters. The presence of small amounts (0.25–0.5% molar) of labeled phospholipid does not influence the shape of compression isotherms either in the absence or in the presence of peptide in the monolayer. Observation of the emitted fluorescence signal is possible either visually or via a low-level video camera. Film balance measurements are controlled through an interfaced personal computer. Video

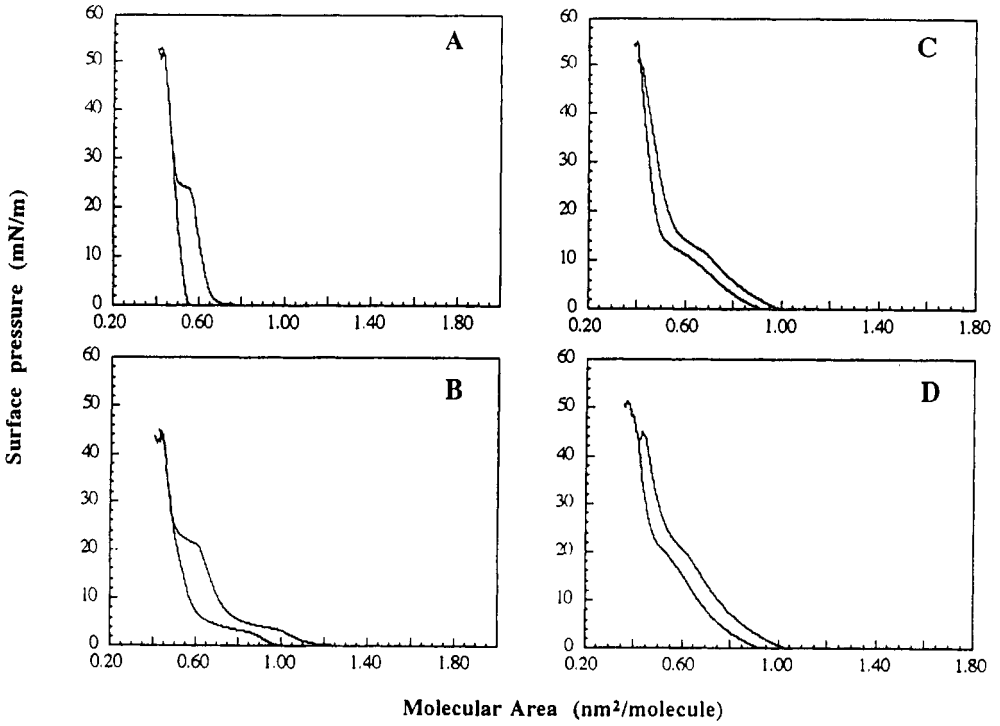

FIGURE 3: Surface pressure/area isotherms of monolayers of L-α-DSPC and L-α-DMPC, at different temperatures, on bombolitin III solutions at different concentrations in Millipore water. In the absence of the lipid the peptide solutions did not display any measurable surface pressure. (A) L-α-DSPC, temperature 25 °C; from left to right the isotherms correspond to 0 and 30 nM bombolitin III. (B) L-α-DSPC, temperature 33 °C; from left to right the isotherms correspond to 0 and 30 nM bombolitin III. (C) L-α-DMPC, temperature 5 °C; from left to right the isotherms correspond to 0 and 30 nM bombolitin III. (D) L-α-DMPC, temperature 15 °C; from left to right the isotherms correspond to 0 and 30 nM bombolitin III.

recording of the monolayer through the video camera was initiated at various time points of film observation. Photographs shown are directly taken from the video screen. The sequence for the experiments at the microscope is as follows: (A) observe after the phospholipid has been spread on the water surface; (B) compress; (C) stop the compression and observe the morphology of the monolayer until an equilibrium is reached (usually in a few minutes); (D) compress again, and so on until there are observations for all parts of the compression isotherm.

Isotherm compression measurements of lipid or lipid–peptide monolayers were taken on a separate Langmuir film balance controlled with a personal computer and equipped with a Wilhelmy plate surface tension measuring system (Albrecht, 1983). Lipid and lipid–peptide films were prepared by spreading small volumes (20–100 μL) of organic solutions of the components, using an Hamilton syringe. For each compression curve at least three separate experiments were performed to check reproducibility. Different compression speeds were also tried to control the reversible behavior of the system.

Kinetic experiments of digestion of monolayers of L-α-DLPC, by PLA_2, were performed using a Langmuir film balance as previously described (Albrecht, 1983). The subphase buffer for these experiments was composed of 10 mM Tris, 20 mM NaCl, and 0.5 mM $CaCl_2$. The buffer was prepared before each experiment by dilution of a 10-fold more concentrated stock solution of the salts, and the pH was adjusted to a value of 8.0 with concentrated HCl. The peptide, bombolitin III, was always dissolved in the water subphase (from a stock solution in water, 0.073 mM) before spreading of the lipid on the surface. Final concentration of the peptide in the subphase was in the range 20–80 nM. After thermal equilibration (25 °C) of the subphase, the lipid was spread on the water surface, and the monolayer was rapidly compressed to obtain a surface pressure of 10 dyn/cm. Once the monolayer showed a constant area behavior, a dilute solution of phospholipase A_2 (3 mL of a stock solution of 2.2 μM PLA_2 diluted to 5 mL with the subphase buffer) was injected slowly under the trough barrier, and the change of the area at constant pressure was followed as a function of time. At least three separate experiments were performed for each peptide concentration in the subphase.

RESULTS AND DISCUSSION

Isothermal Compression Experiments. We followed two different experimental approaches in terms of the mechanism by which the peptide reaches the air–water interface.

(1) The behavior of pure peptide monolayers was studied by dissolving bombolitin III in organic solvent and spreading it directly on the surface of the water subphase. Unfortunately, bombolitin III is not soluble in pure chloroform, so we used a 60:40 $CHCl_3$–MeOH solution as a spreading solvent. It is possible that with this solvent part of the peptide does not remain at the interface because BIII is also very soluble in water. In any case, following this procedure we know the exact amount of peptide that is spread on the water surface and our calculations are based on this value. In Figure 1 we show typical compression isotherms of pure peptide monolayers. The collapse pressure is around 24–26 mN/m, and the limiting molecular area is 250 Å²/molecule when the subphase is pure water. Assuming that all 17 residues of the peptide are organized at the interface, the limiting molecular area per residue is then 14.7 Å², and this value is very close to that (14.2 Å²) reported in the literature for the peptide melittin (DeGrado et al., 1980). Taking into account that bombolitin in different conditions (see CD results) has a content of α-helix around 60–70% and assuming that only the α-helical portion occupies space at the air–water interface,

the limiting molecular area per residue has a value of 22–24 Å^2; this value agrees with that reported for a synthetic amphiphilic docosapeptide designed to mimic the properties of plasma apolipoprotein A-I (Fukushima et al., 1979). These values agree with an orientation of the α-helix axis parallel to the air–liquid interface.

We notice in Figure 1 that at basic pH the compression curve displays a higher limiting molecular area (curve B). In other words, at higher pH the peptide monolayer is less compressible and seems to occupy more space per molecule. This is reasonable since as we go from acidic to basic pH the solubility in water of bombolitin III decreases (the isoelectric point is at pH 10). As mentioned above, we cannot exclude the possibility that at acidic pH part of the peptide, spread on the surface from organic, partitions in the water subphase; this would cause, of course, an apparent higher limiting molecular area for curve A.

(2) To investigate mixed peptide–lipid monolayers, we spread the phospholipid from an organic solvent on the surface of a subphase that consisted of a dilute solution of the peptide (10–100 nM). The alternative would have been to cospread from organic solvent a premixed solution of peptide and phospholipid. It is clear that spreading of both components on the water surface allows better control of the amount of peptide that is present at the interface or at least provides a precise upper concentration limit. On the other hand, as mentioned above, the peptide is not very soluble in chloroform, and we have indications that this solvent can induce the formation of aggregates. For this reason we think that the introduction of bombolitin III in the monolayer by adsorption and penetration from the subphase is more representative of the natural association phenomena of a peptide with a biological membrane than direct spreading of a lipid–peptide mixture from organic solvent. Bombolitin III is positively charged at pH values lower than 8.5–9.0 and is also very soluble in water. Moreover, from previous experiments (Bairaktari et al., 1990b), we know that at these concentrations, in water, the peptide is monomeric and in the random coil conformation. It is clear that with this procedure (adsorption from the subphase) we do not control the amount of peptide that enters the monolayer but instead the system reaches an equilibrium situation in which the monolayer adsorbs a certain amount of peptide as a function of the peptide concentration in the subphase. Given an opportune equilibration time (see below), the mixed monolayer behaves in a reproducible manner and the compression isotherms are reversible.

In Figures 2 and 3 we present a summary of these experiments, with L-α-DPPC and L-α-DSPC at different temperatures. We also performed experiments with shorter alkyl chain phosphatidylcholines, namely L-α-DLPC (data not shown) and L-α-DMPC (Figure 3C,D). With L-α-DPPC we also explored the effect of the pH and the ionic strength of the solution (Figure 4). The results of these experiments can be summarized as follows:

(a) In the absence of the phospholipid monolayer and in the nanomolar concentration range, bombolitin III does not show any signs of surface organization in the pH range 4.5–8.0 in water. As the ionic strength increases and as the pH approaches the isoelectric point of the peptide, bombolitin III shows surface activity and spontaneously organizes at the air–water interface (with no phospholipid present). This is expected since the "salting out" of the hydrophobic side chains will be enhanced when the peptide is less charged and hence less soluble in water.

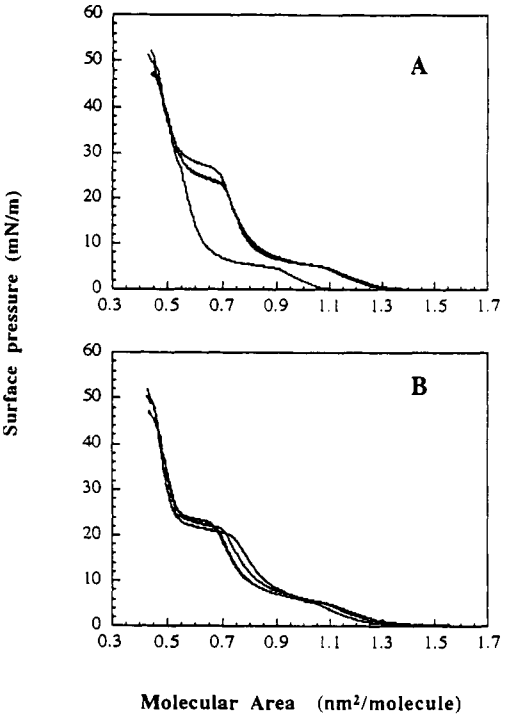

FIGURE 4: Surface pressure/area isotherms of monolayers of L-α-DPPC at 20 °C, at different pH values and ionic strengths. In the absence of the lipid the peptide solutions did not display any measurable surface pressure. (A) Bombolitin III in the subphase at 20 nM. The subphase buffer is 10 mM Tris at pH 6, 7, and 8. The compression isotherm on the far left is for the subphase at pH 7.0 with no peptide. The compression isotherms at pH 6 and 7 are coincident. The compression isotherm at pH 8.0 shows a higher pressure value for the intermediate transition state. (B) Bombolitin III in the subphase at 20 nM. The subphase buffer is 10 mM Tris, pH 7.0, with 1, 2, 5, 10, and 30 mM NaCl. As the salt concentration increases, the collapse pressure for the intermediate state decreases and so does the limiting molecular area (the compression isotherms shift to the right and to lower pressures).

(b) In conditions of zero or very low ionic strength and acidic pH, when the lipid is spread on the water surface, there is always a rapid adsorption of the peptide in the monolayer. The curves shown are taken 0.5–1.0 h after spreading of the lipid. They are reversible and at equilibrium. Some further adsorption of the peptide is also possible (probably diffusion controlled) during a period of several hours.

(c) At all temperatures explored, the mixed monolayers display a two-phase behavior with L-α-DPPC and L-α-DSPC (Figures 2 and 3) and a one-phase behavior with L-α-DMPC (Figure 3) and L-α-DLPC (data not shown). This is similar to and consistent with what was observed by others with melittin (Fidelio et al., 1986), sulfatide and gangliosides (Bianco et al., 1990), myelin basic protein (Bianco et al., 1992), and substance P (Duplaa et al., 1992). If pH and ionic strength can cause the peptide to self-organize at the air–water interface, we notice that the same parameters do not change dramatically the main features of the isotherms of the mixed lipid–peptide monolayers (Figure 4) even though there are minor shifts of the limiting molecular areas and collapse pressures.

Experiments with Uteroglobin Fragments. We also performed experiments (data not shown) with four peptides corresponding to the four helical sequences (4–14, 18–28, 32–47, and 49–65) present in the small globular protein uteroglobin (Morize et al., 1987). The sequence and helical wheel diagrams for these peptides are reported in Table 1. Uteroglobin is a protein isolated from rabbit uterin fluid and was previously shown to be a powerful inhibitor of phospho-

Table 1: Primary Structure and Helical Wheel Diagrams of Bombolitin III and the Four Peptides Corresponding to the Helical Sequences in the Structure of the Protein Uteroglobin

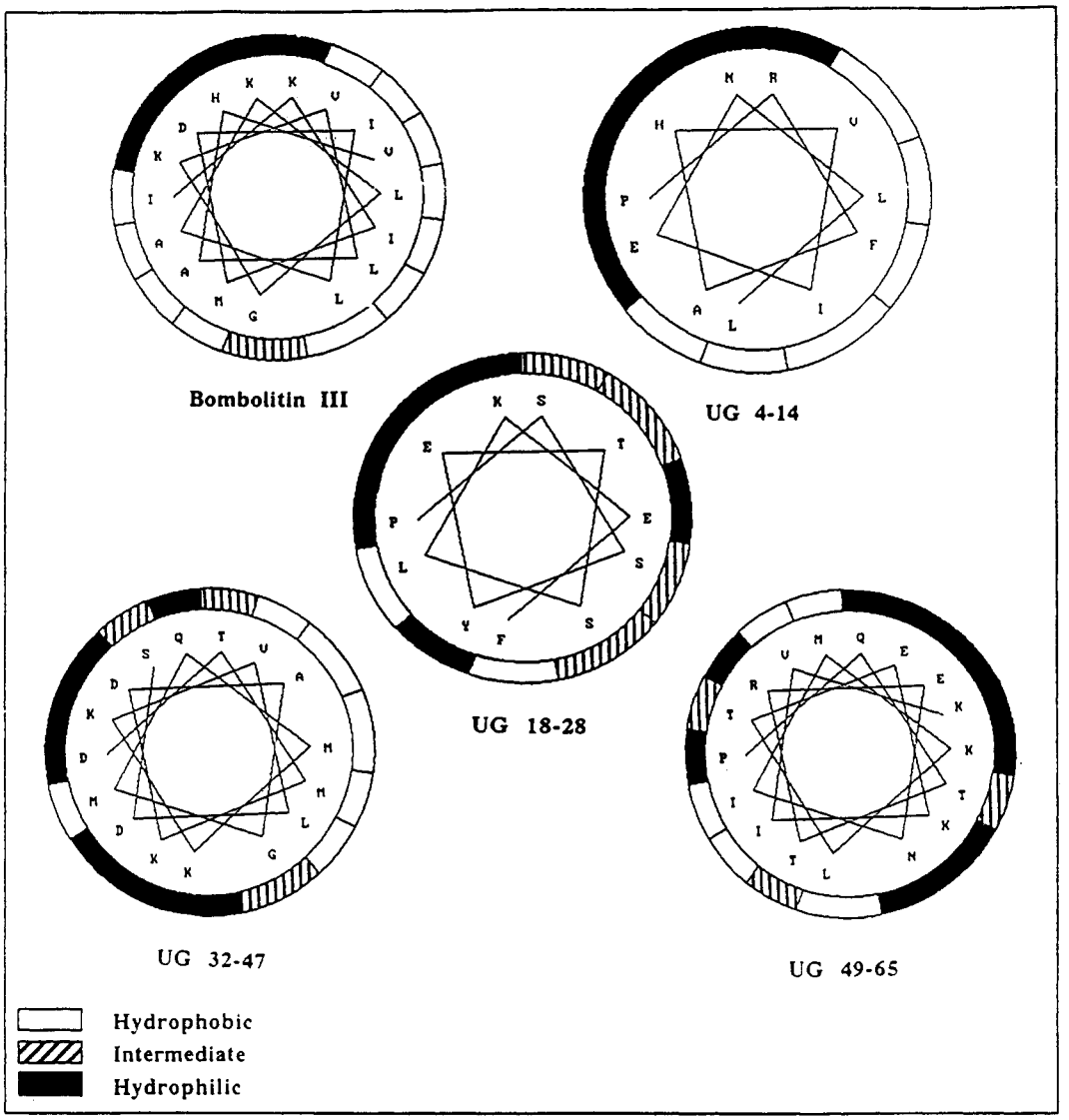

Bombolitin III	Ile-Lys-Ile-Met-Asp-Ile-Leu-Ala-Lys-Leu-Gly-Lys-Val-Leu-Ala-His-Val
UG 4-14	Pro-Arg-Phe-Ala-His-Val-Ile-Glu-Asn-Leu-Leu
UG 18-28	Pro-Ser-Ser-Tyr-Glu-Thr-Ser-Leu-Lys-Glu-Phe
UG 32-47	Asp-Thr-Met-Lys-Asp-Ala-Gly-Met-Gln-Met-Lys-Lys-Val-Leu-Asp-Ser
UG 49-65	Pro-Gln-Thr-Thr-Arg-Glu-Asn-Ile-Met-Lys-Leu-Thr-Glu-Lys-Ile-Val-Lys

lipase A_2 (Brunie et al., 1985). In our laboratory we have synthesized these four peptides and carried out conformational studies in water and in the presence of SDS micelles (Mammi et al., 1992; Tessari et al., 1993). The main reason for the study of these fragments lies in the fact that there have been some conflicting reports (Marastoni et al., 1991; Miele et al., 1988; van Binsbergen et al., 1989) on the capability of a peptide corresponding to helix III in uteroglobin (32–47) to act as an inhibitor of PLA_2.

Our previous experiments (Mammi et al., 1992; Tessari et al., 1993) have indicated that fragment 18–28 (helix II) does not interact strongly with micellar systems, while the other three fragments are able to form partial α-helical structures. We extended these experiments to phospholipid monolayers since these four peptides with variable amphiphilic character (see Table 1) provide a nice comparison term with the properties of bombolitin III. The results indicate that only the short peptide corresponding to helix I (sequence 4–14) has some tendency to be adsorbed in the phospholipid monolayers and at concentrations 10 times higher than those of bombolitin III. The other three peptides do not penetrate the monolayer at all. In fact, peptide 4–14 is the only one of the four that has a well-defined amphiphilic character when structured as an α-helix. This finding confirms that the interaction with the monolayer is not possible with just any peptide sequence in which both apolar and charged polar side chains are present. It appears that the adsorption in the monolayer is possible only if the amphiphilic structure is very well-defined (BIII and fragment 4–14). Moreover, the phospholipid monolayer seems to be a more selective system,

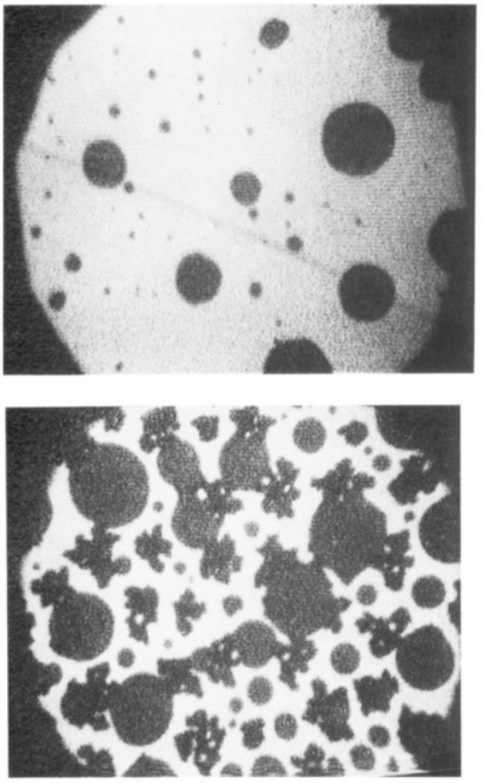

FIGURE 5: Real time epifluorescent observation (sulforhodamine filter) of L-α-DPPC monolayer on subphase of bombolitin III (35 nM) solution in 150 mM Tris buffer, 10 mM NaCl, and 5 mM $CaCl_2$, temperature 25 °C. (A) Formation of phase-separated domains of bombolitin III (surface pressure = 2 mN/m). (B) Upon compression, solid L-α-DPPC domains crystallize around the peptide domains (surface pressure = 13 mN/m).

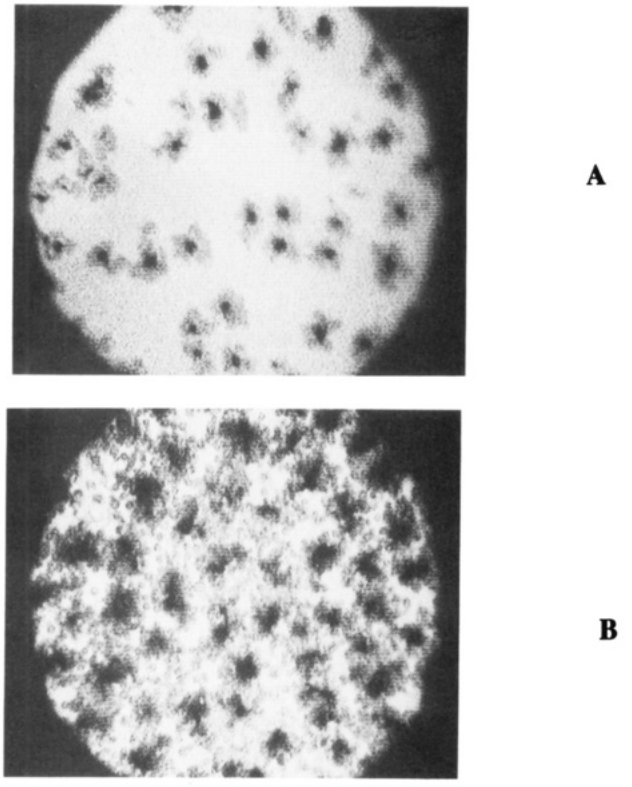

FIGURE 6: Real time epifluorescent observation (sulforhodamine filter) of L-α-DPPC monolayer on subphase of bombolitin III (73 nM) in Millipore water at 25 °C. (A) Formation of pure L-α-DPPC solid domains and around them gray domains of bombolitin III (surface pressure = 10 mN/m). (B) Same as in (A) after compression to surface pressure of 14.5 mN/m.

compared to SDS micelles, since fragments 32–47 and 49–65 form helical structure with micelles (Mammi et al., 1992; Tessari et al., 1993) but do not interact with monolayers even at concentration 100 times higher than that of bombolitin III.

Fluorescence Microscopy of Peptide–Lipid Monolayers. The results exposed in the previous section are consistent with a very high affinity of bombolitin III for phospholipid monolayers and show that even though this affinity is clearly higher in the conditions in which the peptide is less water soluble (basic pH and increasing ionic strength), the peptide is strongly adsorbed in the monolayers even in the conditions in which it is very soluble in water. This would be difficult to explain if the peptide did not undergo a conformational transition that geometrically separates the hydrophobic from the hydrophilic or charged residues. The isothermal compression experiments give a good indication of the presence (with L-α-DPPC or L-α-DSPC) or absence (with L-α-DLPC or L-α-DMPC) of the phase separation phenomena. To obtain further information on the kind of organization that is taking place in the mixed monolayers, we decided to observe them with the epifluorescence microscope. In the case of monolayers that do not show the phase separation phenomena (with either L-α-DMPC or L-α-DLPC as the phospholipid component) the analysis at the microscope confirms that the peptide is homogeneously mixed with the lipid, since only a homogeneous fluorescence is observed. Very different are the results for the phase-separated mixed monolayers (with either L-α-DPPC or L-α-DSPC as the phospholipid component). In Figure 5 we show an experiment in which L-α-DPPC was spread on the surface of a subphase containing bombolitin III. The subphase consisted of a typical buffer used for PLA_2 activity assays (150 mM, 10 mM NaCl, 5 mM $CaCl_2$, pH 8.0). One hour after spreading (Figure 5A), we can clearly see organized domains at a pressure value where lipid alone would still be in the liquid analogous state. These circular shape domains are clearly composed of the phase-separated peptide that has been adsorbed at the monolayer. Careful observation shows that they are not completely dark, and this indicates that they contain some phospholipid, doped with the fluorescent probe. When the monolayer is compressed, these domains are stable and they do not increase their size; rather we see that some pure lipid solid domains start to crystallize around and inside the peptide–lipid domains (Figure 5B). This kind of behavior (Figure 5) is generally displayed when the subphase is at pH 8–9 and the ionic strength is above 100 mM.

In the case of a water subphase at pH lower than 6 and with low ionic strength, we observe a different behavior that is reported in Figure 6. In this case, after spreading of the lipid (L-α-DPPC), we do not observe the initial formation of the peptide gray domains. Only after compression (Figure 6A) do we start to see the formation of black solid domains, probably composed of pure lipid (but we cannot exclude the incorporation of some peptide into them). Almost at the same time around the black lipid domains we notice the formation of other solid domains, partly bright, that are very probably mainly composed of peptide mixed with some lipid (Figure 6B). Thus, under these conditions we have an organization that seems to be reversed compared to the situation at basic pH with salt; in this case the formation of BIII domains is induced by the formation of lipid domains.

In Figure 7 we see another experiment performed at high pH with L-α-DSPC at 35 °C; the behavior is similar to that observed with L-α-DPPC (Figure 5). We have an initial formation of peptide phase-separated domains, and upon compression pure lipid (black dots) crystallizes around and

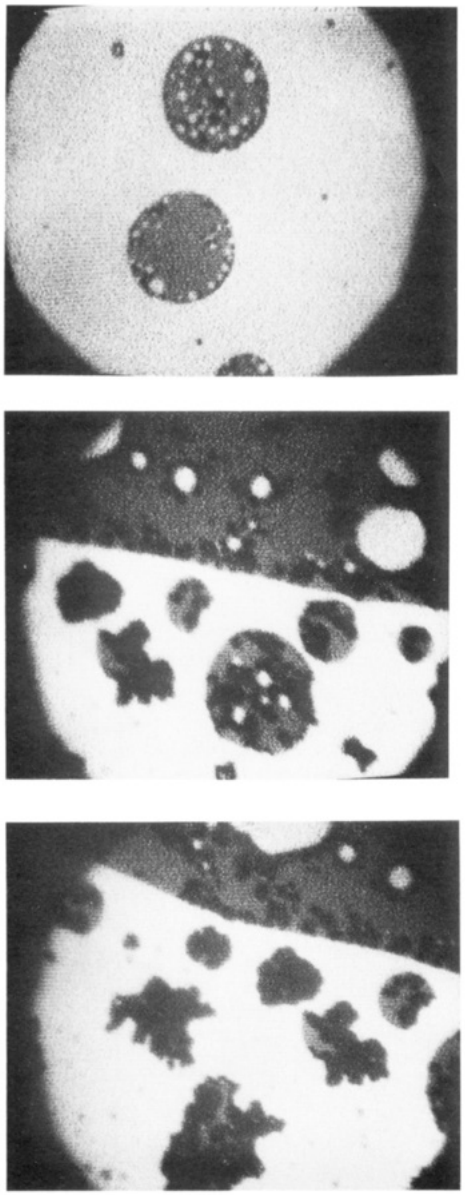

FIGURE 7: Real time epifluorescent observation (sulforhodamine filter) of L-α-DSPC monolayer on subphase of bombolitin III (36.5 nM) in Millipore water at 35 °C. (A) Formation of phase-separated domains of bombolitin III (surface pressure = 1 mN/m). (B and C) Upon compression to 2.5 mN/m there is formation of solid L-α-DSPC domains around and inside the peptide domains.

inside the peptide–lipid domains. Under these conditions (higher temperature) the percentage of pure lipid in the mixed peptide–lipid domains is higher than in the case of L-α-DPPC at 25 °C (Figure 5B) since a lot of small black solid lipid crystals are formed inside the gray domains (Figure 7B,C).

It is important to notice that changing the subphase conditions, in terms of pH and ionic strength, causes only minor changes in the shape of the isothermal compression curves (Figure 4). The microscope observation, on the other hand, tells us that there are drastic changes in the microscopic organization of the peptide–lipid mixed monolayer.

Fluorescence Microscopy: Interaction of PLA_2 with Mixed Monolayers. The epifluorescence microscope technique was used previously (see introduction) to investigate the action of phospholipase A_2 on the phospholipid monolayers. In particular, it was possible to visualize how this enzyme preferentially acts at the liquid–solid interface of phospholipid monolayers in their phase transition region. In this respect it was interesting to investigate the action of this enzyme on the mixed bombolitin III–L-α-DPPC monolayers. The subphase needed for the enzyme to be active is at pH 8.0 and with NaCl between 20 mM and 0.15 M; under these conditions we have shown that the peptide forms phase-separated domains and upon compression pure lipid crystallizes around the peptide domains. In Figure 8 we show an experiment (with L-α-DPPC) in which the subphase at pH 8.0 has an ionic strength above 150 mM. These are conditions similar to the experiment shown in Figure 5. After the initial observation of the peptide circular domains, upon compression we have the crystallization of pure lipid around the peptide–lipid domains (Figure 8A). By observing the same monolayer (Figure 8B) through the FITC filter we can better distinguish the double composition of the domains: a central part, which is mainly peptide, surrounded by pure lipid. After formation of these solid lipid–peptide domains, the enzyme was injected in the subphase. It is clear that the enzyme is active on this mixed monolayer, and as the lipolysis proceeds we observe the following:

(a) The solid lipid domains around the peptide domains (Figure 8C) change their morphology; the lipid forms droplet-shaped structures at the border of the peptide domains.

(b) As the lipolysis proceeds (30 min), the lipid domains that surround the peptide domains open up (Figure 8D) and the peptide domains seem to disaggregate; hence, as the monolayer becomes richer in lipolysis products (lysolecithin and fatty acid), the peptide domains are not stable anymore. In addition, it can be seen that phase-separated peptide domains that are not totally surrounded by solid analogous lipid are disaggregating earlier.

(c) After about 60 min (Figure 8E), there are no longer visible peptide phase-separated domains; only the partially hydrolyzed lecithin in a homogeneous monolayer of lecithin, lysolecithin, fatty acid, and peptide are observable. Since the pressure remains constant during the hydrolysis reaction, the disappearance of the bombolitin III domains seems to be due to a better miscibility of the peptide in the new composition of the monolayer and not to a migration of peptide molecules from the monolayer into the subphase.

(d) After more than 80 min and using fluorescein-labeled PLA_2, the formation of enzyme domains can be observed via the FITC filter (Figure 8F); this is in agreement with the original investigations of the activity of PLA_2 on lipid monolayers (Ahlers et al., 1990; Grainger et al., 1990a).

In Figure 9 we show a similar experiment with PLA_2, but in this case the subphase at pH 8.0 has a lower ionic strength (around 30 mM). The conditions are then similar to those of the experiment in Figure 6. At the beginning, after spreading of the lipid (L-α-DPPC), we do not observe the formation of peptide domains. Upon compression (Figure 9A–C) one finds the formation of lipid solid analogous domains, and at the same time also the peptide displays phase separation (gray domains). At this point the enzyme was injected in the subphase, and after approximately 20 min (Figure 9D), we observed the complete disappearance of the peptide domains, as in the previous experiment (Figure 8E).

It would be very difficult, with this technique, to quantify if there is a kinetic effect of activation due to the presence of the peptide. What we notice is that the peptide domains all disappeared after approximately 0.5–1.0 h of reaction, leaving behind still pure lipid solid domains. The global reaction time for the complete digestion is of the order of 2 h with and without the peptide in the monolayer. Certainly it seems that the change in composition of the monolayer (due to the lipolysis), which causes the peptide to disaggregate, is on a shorter time scale than the normal times required for PLA_2

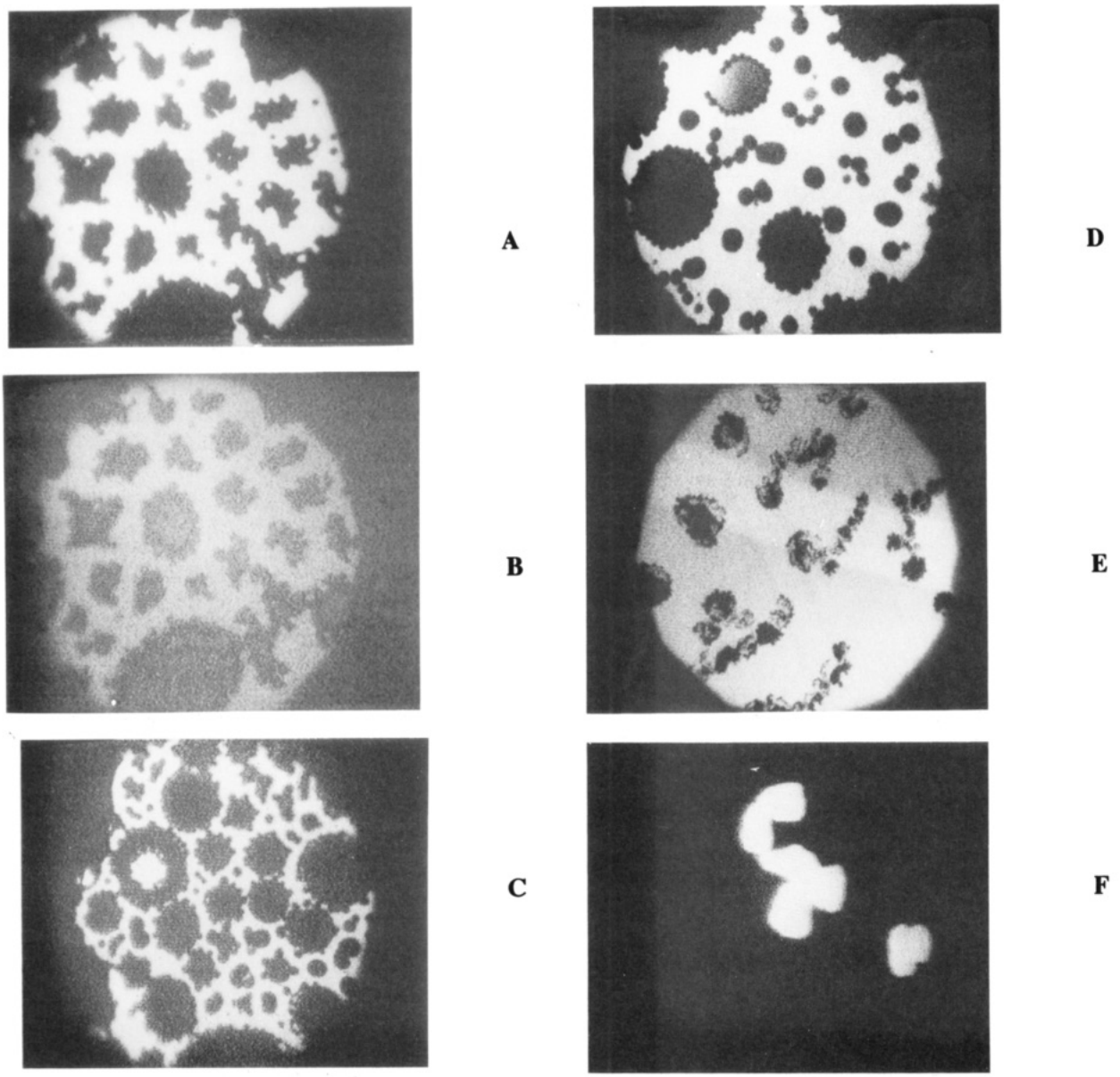

FIGURE 8: Real time epifluorescent observation (sulforhodamine filter) of L-α-DPPC–bombolitin III mixed monolayer hydrolysis by PLA_2. Subphase buffer is 10 mM Tris, 0.15 M NaCl, 5 mM $CaCl_2$, pH 8.0, temperature 25 °C. (A) Before PLA_2 injection (surface pressure = 2–3 mN/m), monolayer shows the presence of the double-composition domains. (B) As in (A) but looking through the FITC filter. (C) Twenty minutes after PLA_2 injection; formation of droplet structures of the pure lipid crystals. (D) Thirty minutes; the peptide domains start to disaggregate. (E) One hour; all of the peptide domains have disappeared; surface pressure remains constant at 2–3 mN/m. (F) Eighty minutes; formation of PLA_2 aggregated domains; observation through the FITC filter.

to digest a monolayer with no peptide, and this might indicate that the lipid domains are attacked by the enzyme more rapidly if BIII is present. This effect is interesting since we also demonstrate by a different kinetic experiment (next section) that indeed the presence of bombolitin III in L-α-DLPC monolayers increases the initial speed of lipolysis.

Effect of BIII on the Activity of PLA_2. We have shown above that bombolitin III is able to organize itself at the air–water interface and that it is also able to spontaneously partition in a monolayer film of pure phospholipid, from a very dilute water solution. We also prove (next section, CD measurements) that bombolitin III interacts with phospholipid vesicles via a conformational transition to an α-helical secondary structure. Bombolitin III has been reported (Argiolas & Pisano, 1985) to increase the activity of different phospholipases A_2, toward egg yolk lecithin liposomes, in an in vitro assay based on the release of arachidonic acid. We decided to quantify the effect of BIII on the speed of hydrolysis of monolayers of pure lipid. For these experiments we used monolayers of L-α-DLPC: the hydrolysis products are soluble in the water subphase and, as a consequence, as the reaction proceeds there is a drop in the surface pressure of the monolayer. By keeping the pressure constant, it is possible to follow the course of the enzymatic reaction by recording the values of the surface area as a function of time (Grainger et al., 1990b).

The peptide was dissolved in the water subphase at a concentration ranging between 20 and 80 nM. Immediately after the lipid is spread on the water subphase, one observes an adsorption of the peptide at the monolayer; this shows up as an increase in pressure that ranges from 1 mN/m for 20 nM BIII to 2.5–3.0 mN/m for 80 nM BIII. All of the experiments were performed at the same total value of surface pressure (10 mN/m) because it is well documented (Hall, 1992; Verger & de Haas, 1976) that the rate of lipolysis is surface pressure dependent and exhibits a maximum around 12 mN/m. After the initial increase in pressure due to the peptide adsorption, the monolayer is compressed to reach a

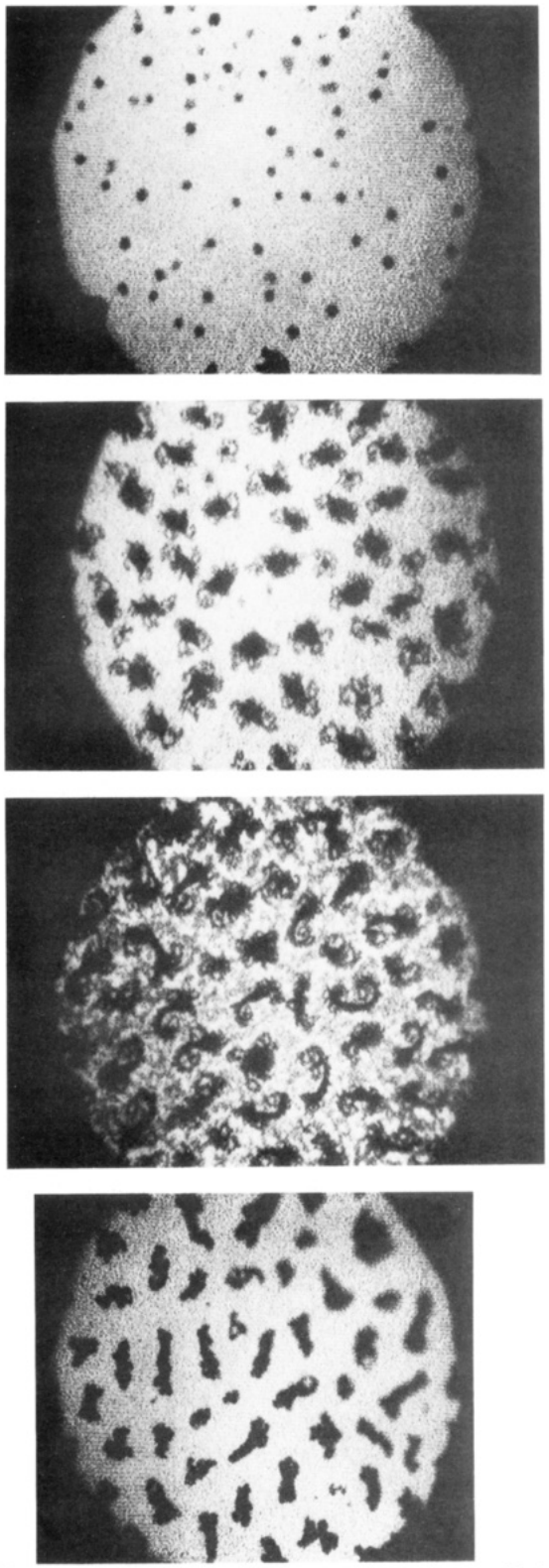

FIGURE 9: Real time epifluorescent observation (sulforhodamine filter) of L-α-DPPC–bombolitin III mixed monolayer hydrolysis by PLA_2. Subphase buffer is 10 mM Tris, 20 mM NaCl, 0.5 mM $CaCl_2$, pH 8.0, temperature 25 °C. (A–C) Before PLA_2 injection; sequence shows the compression of the monolayer. At low pressure (A, 15 mN/m) no phase-separated peptide domains are observable; increasing pressure (B, 17.5 mN/m; C, 19 mN/m) brings the formation of pure lipid solid domains and also peptide gray domains. (D) Twenty minutes after PLA_2 injection, all of the peptide domains have disappeared.

surface pressure value of 10 mN/m (including the increase in pressure due to the peptide adsorption). After an equilibration period ranging between 15 and 30 min, during

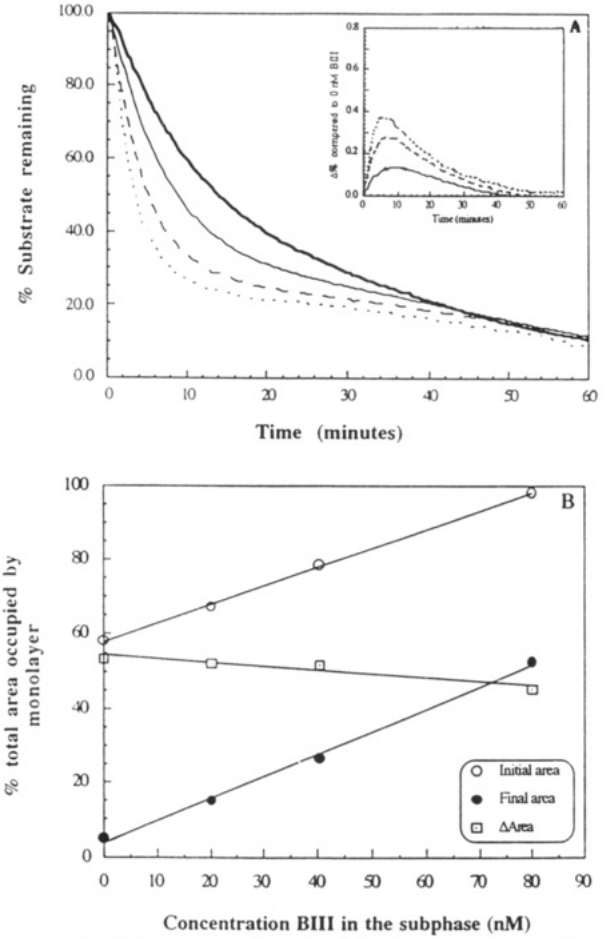

FIGURE 10: Time course of the hydrolysis of monolayers of L-α-DLPC with PLA_2 at 25 °C and constant surface pressure of 10 mN/m. The subphase buffer is 10 mM Tris, 10 mM NaCl, and 2 mM $CaCl_2$. The subphase contained bombolitin III at 0 (—), 20.3 (—), 40.6 (– – –), and 80 nM (- - -). (A) Graph of the percentage of substrate remaining in the monolayer as a function of time. In the inset are shown difference plots between the curves in the presence of peptide and the reference curve with no peptide. (B) Graph of the values (100% corresponds to the maximum available area) of the initial and final (after digestion) areas of the monolayer as a function of the peptide concentration in the subphase.

which the area stabilizes to a constant value, phospholipase A_2 is injected in the subphase from under the trough barrier. The digestion begins immediately with no lag period, and the area value as a function of time is recorded automatically. In Figure 10A we show the results of such experiments. The raw data have been elaborated to plot the percentage of substrate (L-α-DLPC) remaining in the monolayer on the assumption that the area decrease is only due to the digestion of the substrate and not to an eventual desorption of the peptide. We think that this is a valid assumption since compression isotherms performed before and after the digestion show that the peptide, once it is adsorbed, remains organized at the air–water interface. Figure 10A shows that in the presence of bombolitin III adsorbed in the monolayer the lipolysis proceeds more quickly. Since the surface pressure is always kept at the same value, the initial and final values of the total area are larger in the presence of increasing peptide concentrations in the subphase. We report in Figure 10B a plot of the surface area (at a pressure of 10 mN/m) as a function of peptide concentration in the subphase. There is a good proportionality relation between the peptide concentration and the amount of peptide adsorbed at the interface. Also, the Δ area value, corresponding to the total area occupied by the lipid, is approximately constant. It is worth pointing out

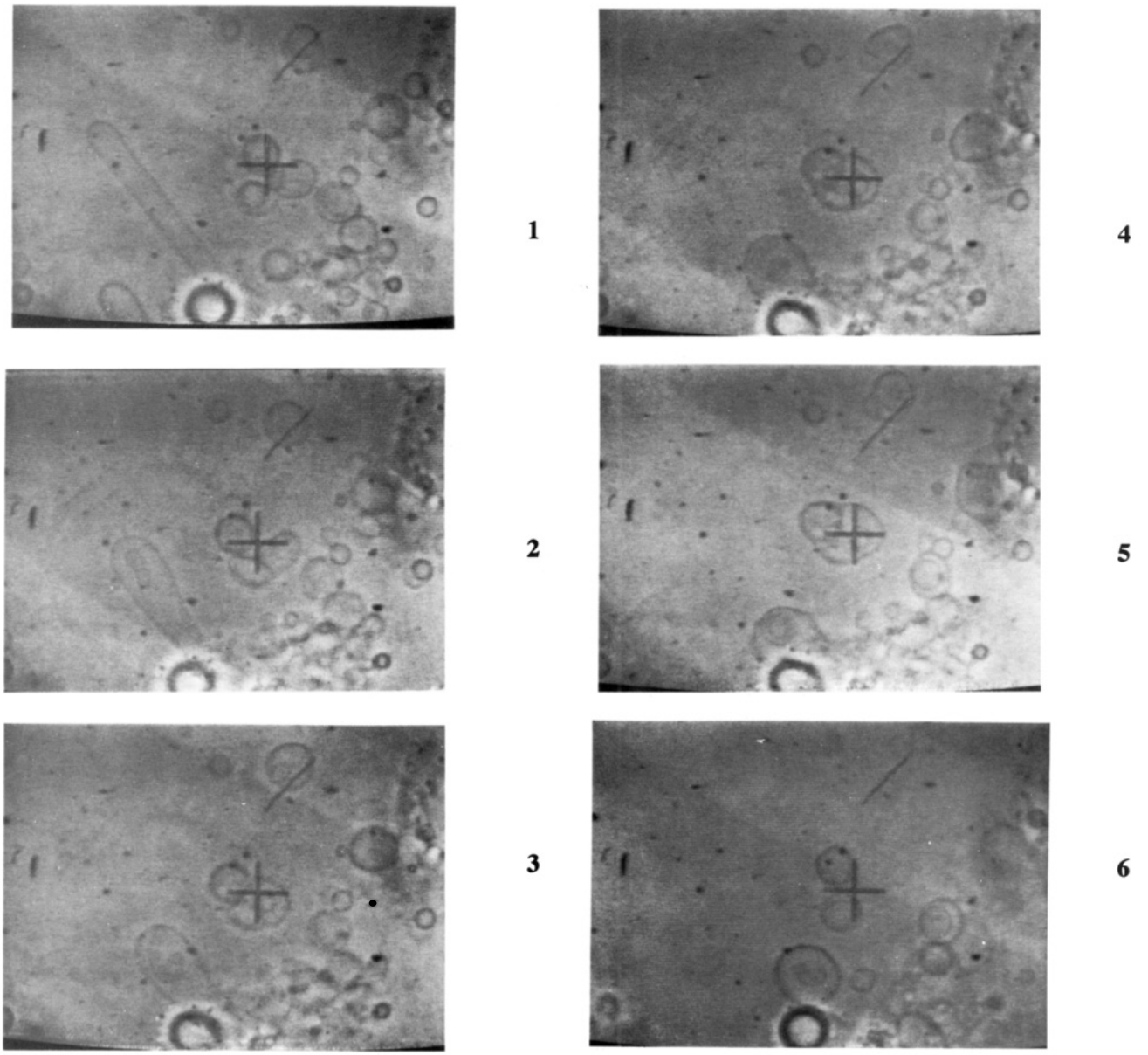

FIGURE 11: Inverse microscope observation of the effect of bombolitin III (0.15 mM) on the morphology of tubelike and circular liposomes of L-α-DMPC in 10 mM NaCl, temperature 30 °C. The series of photographs was taken at intervals of 20–30 s after injection of the peptide solution.

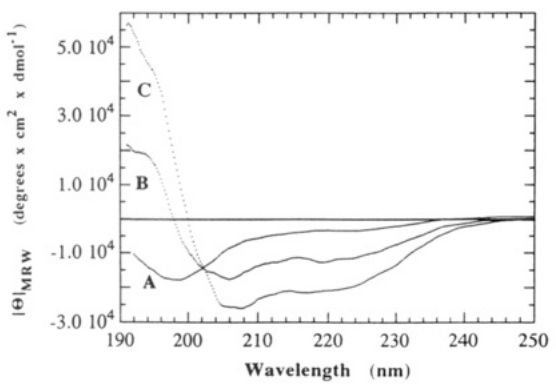

FIGURE 12: Circular dichroism spectra of bombolitin III in aqueous solution (22.75 μM) with increasing concentration of L-α-DMPC small unilamellar vesicles, temperature 25 °C. L-α-DMPC monomer concentration is (A) 0.3, (B) 1.96, and (C) 5.3 mM.

that the activation effect of the peptide in the monolayer is visible despite the dilution of the lipid substrate that occurs as a consequence of the increase of the total area at which the reaction takes place. In the inset in Figure 10A we show the difference between the kinetic curves obtained in the presence and in the absence of peptide in the subphase. It is clear from this figure that the increase in lipolysis speed is not constant but reaches a maximum at a time of approximately 10 min. We do not think that this effect is related to the action of bombolitin III but is possibly due to the dilution of the substrate in the monolayer. In the absence of peptide the enzyme is faced with a constant composition monolayer at all times of the reaction. When the peptide is in the monolayer, at the beginning of the reaction the enzyme finds enough lipid to digest and, despite the dilution effect, bombolitin displays an activation, but as the reaction proceeds the dilution effect overcomes the activation effect and the lipolysis speed is diminished.

These results are in agreement with the previous findings of Argiolas and Pisano, but we show that the peptide performs its effect on the activity of the enzyme by mixing with the substrate and modifying its physical state. We also performed some trials to see the effect of the short sequence 4–14 of uteroglobin on the activity of PLA_2. This short peptide was previously shown to be able to adopt an α-helical structure in

the presence of SDS micelles (Mammi et al., 1992; Tessari et al., 1993) and in this conformation has a well-defined amphiphilic character (see Table 1). Despite the fact that this peptide, similarly to bombolitin III, is adsorbed in the monolayer, we did not find variation of the lipolysis speed in this case. This negative result is interesting since it shows that amphiphilicity and adsorption in the monolayer are not sufficient conditions to determine an effect on the enzymatic activity. Further experiments will be necessary to precisely determine the role of other factors such as the length of the helix and the presence of charged side chains.

Interaction of BIII with Giant and Small Liposomes. All of the experiments described in the preceding sections were performed on phospholipid monolayers. To complete this study, we also investigated the interaction of bombolitin III with lecithin (L-α-DMPC) double-layer giant and small liposomes.

In a first set of experiments it was necessary to clarify whether the peptide interacts with the liposomes via the formation of an α-helical structure or is also able to interact in its random conformation. To solve this problem, we performed some CD spectroscopy experiments with preparations of small unilamellar vesicles (it is not possible to work with large liposomes because of the heavy light scattering). The results are shown in Figure 12: the three spectra shown demonstrate that as the SUV concentration increases, the peptide goes from the random coil conformation (predominant in pure water at this peptide concentration) to the α-helical conformation. The presence of an isodichroic point confirms that the system is two-state; the peptide in water is random coil, and the peptide associated with the vesicles is α-helical.

To directly visualize the effect of BIII on double layers, giant liposomes (10–50 μM) were used as a model for the membrane system. Liposomes of this size can be easily observed with a light microscope connected to a video camera (Decher et al., 1980). The photographs shown in Figure 11 are taken directly from the video screen. The liposomes shown are prepared by swelling of a film of L-α-DMPC in 10 mM NaCl at 30 °C, above the critical temperature for this particular phospholipid. Before a solution of bombolitin III was injected, in the flow chamber, the liposomes were kept under observation for several hours to control the stability of their structure; in this way we ensure that the effect seen is due to interaction with the peptide. The photographs in Figure 11 represent the effect on the liposomes after injection of a bombolitin III solution; the sequence is taken over a period of 1–2 min and shows that tubelike liposomes collapse to a circular structure and circular liposomes also are made more unstable and either collapse or fuse with other liposomes nearby. The effect of the peptide is most likely due to the insertion of hydrophobic side chains in the outer layer of the liposomes.

Conclusions. In this work we have applied a number of different techniques to characterize the interaction of a natural amphiphilic peptide with phospholipidic systems useful as models of the cellular membrane. This varied approach is necessary since several questions remain open on the real nature of the action of these "toxin" peptides and their effect on membrane enzymes.

It seems well accepted that bombolitins and other similar, biologically active, peptides interact with the membrane through the formation of amphiphilic secondary structures. In this way they associate and mix with the membrane, and their presence in the membrane structure is able to influence, for example, the activity of phospholipase A_2. It is still not clear, though, if the enzyme is activated simply because the membrane is in a different physical state (for example, more fluid or more disordered) when the peptide is present or if there is also a more direct effect of the peptide (in the membrane) on the enzyme. One could think, for example, that microdomains of the peptide create, in the membrane, an interface at which the lipolysis proceeds more quickly or that a favorable electrostatic interaction between the peptide and the enzyme takes place that will stabilize and favor the activity of the protein associated with the membrane. We are planning to answer these questions by studying a surface active bombolitin analog in which the charge will be negative or less positive.

Our experiments show that Langmuir film balance techniques alone are not sufficient to give a complete picture of the organization of the peptide at the interface; specifically, using the fluorescence microscope, we have been able to detect the presence of peptide "domains" and to follow the lipid crystallization on these domains. Further experiments in this sense will involve the labeling of the peptide with a fluorescent probe to be able to visualize pure monolayers of peptide and to better analyze the behavior of mixed monolayers with phospholipids.

REFERENCES

Ahlers, M., Muller, W., Reichert, A., Ringsdorf, H., & Venzmer, J. (1990) *Angew. Chem., Int. Ed. Engl. 29*, 1269–1285.

Albrecht, O. (1983) *Thin Solid Films 99*, 227–234.

Argiolas, A., & Pisano, J. J. (1985) *J. Biol. Chem. 260*, 1437–1444.

Bairaktari, E., Mierke, D. F., Mammi, S., & Peggion, E. (1990a) *Biochemistry 29*, 10090–10096.

Bairaktari, E., Mierke, D. F., Mammi, S., & Peggion, E. (1990b) *Biochemistry 29*, 10097–10102.

Bianco, I. D., Fidelio, G. D., & Maggio, B. (1990) *Biochim. Biophys. Acta 1026*, 179–185.

Bianco, I. D., Fidelio, G. D., Yu, R. K., & Maggio, B. (1992) *Biochemistry 31*, 2636–2642.

Brunie, S., Bolin, J., Gewirth, D., & Sigler, P. B. (1985) *J. Biol. Chem. 260*, 9742–9749.

Decher, G., Kuchinka, E., Ringsdorf, H., Venzmer, J., Bitter-Suermann, D., & Weisberger, C. (1980) *Angew. Makromol. Chem. 166/167*, 71–80.

DeGrado, W. F., Kezdy, F. J., & Kaiser, E. T. (1980) *J. Am. Chem. Soc. 103*, 679–681.

Duplaa, H., Convert, O., Sautereau, A. M., Tocanne, J. F., & Chassaing, G. (1992) *Biochim. Biophys. Acta 1107*, 12–22.

Fidelio, G. D., Maggio, B., & Cumar, F. A. (1986) *Biochim. Biophys. Acta 862*, 49–56.

Fukushima, D., Kupferberg, J. P., Yokoyama, S., Kroon, D. J., Kaiser, E. T., & Kezdy, F. J. (1979) *J. Am. Chem. Soc. 101*, 3703–3704.

Grainger, D. W., Reichert, A., Ringsdorf, H., & Salesse, C. (1989) *FEBS Lett. 252*, 73–82.

Grainger, D. W., Reichert, A., Ringsdorf, H., & Salesse, C. (1990a) *Biochim. Biophys. Acta 1023*, 365–379.

Grainger, D. W., Reichert, A., Ringsdorf, H., Salesse, C., Davies, D. E., & Lloyd, J. B. (1990b) *Biochim. Biophys. Acta 1022*, 146–154.

Hall, D. G. (1992) *Biochem. J. 287*, 73–78.

Kaiser, E. T., & Kezdy, F. J. (1983) *Proc. Natl. Acad. Sci. U.S.A. 80*, 1137–1143.

Litman, B. J. (1972) *Biochemistry 11*, 3243–3247.

Mammi, S., Foffani, M. T., Improta, S., Tessari, M., Schievano, E., & Peggion, E. (1992) *Biopolymers 32*, 341–346.

Marastoni, M., Salvadori, S., Balboni, G., Scaranari, V., Santagada, V., Romualdi, P., Ferri, S., & Tomatis, R. (1991) *Arzneim. Forsch. 41*, 240–243.

Meller, P. (1988) *Rev. Sci. Instrum. 59*, 2225–2231.
Miele, L., Cordella-Miele, E., Facchiano, A., & Mukherjee, A. B. (1988) *Nature 335*, 726–730.
Morize, I., Surcouf, E., Vaney, M. C., Epelboin, Y., Buehner, M., Fridlansky, F., Milgrom, E., & Mornon, J. P. (1987) *J. Mol. Biol. 194*, 725–739.
Reichert, A., Ringsdorf, H., & Wagenknecht, A. (1992) *Biochim. Biophys. Acta 1106*, 178–188.
Ringsdorf, H., Schlarb, B., & Venzmer, J. (1988) *Angew. Chem., Int. Ed. Engl. 27*, 113–158.
Szoka, F., Jr., & Papahadjopoulos, D. (1980) *Annu. Rev. Biophys. Bioeng. 9*, 467–508.
Tessari, M., Foffani, M. T., Mammi, S., & Peggion, E. (1993) *Biopolymers 33*, 1877–1887.
van Binsbergen, J., Slotboom, A. J., Aarsman, A. J., & de Haas, G. H. (1989) *FEBS Lett. 247*, 293–297.
Verger, R., & de Haas, G. H. (1976) *Annu. Rev. Biophys. Bioeng. 5*, 77–117.
Wallace, B. A., & Blout, E. R. (1979) *Proc. Natl. Acad. Sci. U.S.A. 76*, 1775–1779.
Wallace, B. A., Veatch, W. R., & Blout, E. R. (1981) *Biochemistry 20*, 5754–5760.